9TH INTERNATIONAL CONFERENCE ON COMPOSITE CONSTRUCTION IN STEEL AND CONCRETE
M. Knobloch, U. Kuhlmann, W. Kurz, M. Schäfer. (Eds.)
Online, Germany, July 27-29, 2021

ENGINEERING MODEL FOR THE VERTICAL SHEAR CAPACITY OF COMPOSITE SLABS WITH ADDITIONAL REINFORCING STEEL

Nicole Schmeckebier*, Wolfgang Kurz**

* KREBS+KIEFER Ingenieure GmbH Köln
e-mail: schmeckebier.nicole@kuk.de

** Technische Universität Kaiserslautern
e-mail: wolfgang.kurz@bauing.uni-kl.de

Keywords: Composite Slabs, Shear Capacity, Engineering Model, Design, Standards, Experimental Investigations.

Abstract. *Up to now, no independent model for the shear design of composite slabs under the consideration of the two types of longitudinal reinforcement – metal sheet and reinforcing steel – exists. Therefore, extensive investigations were conducted at Technische Universität Kaiserslautern. The research project was completed recently. A new engineering model, which was calibrated on tests, was developed. Furthermore, the engineering model was transferred into a design model. In this paper the experimental investigations are presented as well as the engineering model.*

1 INTRODUCTION

Eurocode 4 [1] says that the shear capacity of composite slabs should be calculated according to Eurocode 2 [2] by using the empirical supported formula of concrete slabs without shear reinforcement. This formula refers on the one hand to the tooth model from Reineck [3] and on the other hand to the analysis of an extensive data base of shear tests on concrete specimen [4]. This model is based on some assumptions that are not valid for composite slabs. The metal sheet has its own shear capacity and the dowel effect of the slab is weaker than the dowel effect of the reinforcing steel. Furthermore, the bond stiffness of metal sheets is significantly lower than that of reinforcing steel. In addition, there is the fact that the empirical formula of Eurocode 2 [2] was determined by analysis of an extensive database of shear tests only on concrete specimen.

Furthermore, a lack of security for the calculation of the shear capacity of composite slabs made of lightweight concrete was noticed in [5]. In this paper tests on composite slabs are described, whereby the aim of this research was the investigation of the longitudinal bond action. The observed failure mode was a combination of longitudinal shear and transverse shear failure. Therefore, a new design model for the shear capacity of composite slabs without additional reinforcement [6] was developed at Technische Universität Kaiserslautern. This design model is valid for composite slabs made of lightweight concrete as well as normal concrete, but the main focus of this research project were the studies on specimens with lightweight concrete. The model contains three mechanisms that act additive. The shear capacity of the metal sheet and the bearing capacity of the uncracked compression zone together are described as the basic value because they act permanently. A third mechanism, the tensile bearing effects in the crack tip, can be added for re-entrant profiles. This shape guarantees an effective bond action so that critical crack width can be avoided.

In practice, composite slabs are mostly built with additionally reinforcement. But the significant influence of the reinforcing steel cannot be considered entirely in the model of [6]. Therefore, further research was necessary.

2 EXPERIMENTAL INVESTIGATIONS

2.1 General

In general, shear failure doesn't occur in composite slabs. So, the enforcement of shear failure in tests is very difficult. Therefore, the specimens were designed as small stripes of slabs and with uncommon dimensions. Two cross sections are shown as an example in figure 1. To avoid longitudinal shear failure an effective end anchorage was used. As reinforcing steel threaded anchor bars made of high strength steel [7] with a diameter of 15 mm were used to increase the bending capacity compared to the shear capacity disproportionately. In accordance with the rules, the reinforcing steel was placed as mesh reinforcement directly on the top of the metal sheet. In each rib one rebar was located and normal concrete C30/37 was used. The test setup was realised as a three-point-bending-test with an offset arrangement of the load. The distance between the support and the load introduction was set to three times of the effective height d_m. The width of the specimens corresponded to twice of the ribs of the metal sheet.

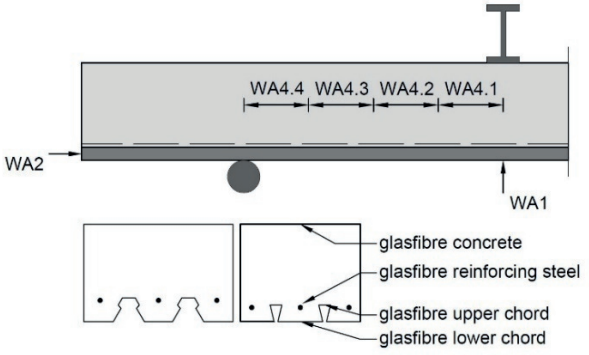

Figure 1. Schematic representation of cross sections of specimens and arrangement of measurement.

Table 1: Overview of combination of parameters of tests and failure loads of tests.

combination [-]	metal sheet [-]	thickness of metal sheet [mm]	height [mm]	width [mm]	f_{ctm} [N/mm²]	f_{cm} [N/mm²]	reinforcement [-]	V_{test} [kN]
1	SHR [8]	1.00	300	370	2.1	24.4	Ø15/15	168.0|137.2
2	C70 [9]	1.00	300	460	2.1	24.4	Ø15/18	172.2|185.6
3	Hody [10]	1.00	280	500	2.0	24.9	Ø15/20	178.9|164.0
4	ComFlor 80	1.00	280	690	2.0	24.9	Ø15/30	248.9|249.6
5	Hody [10]	0.75	280	500	2.4	27.8	Ø15/20	209.4|180.3
6	SHR [8]	0.75	300	370	2.4	27.8	Ø15/15	139.9|157.3
7	SHR [8]	1.25	300	370	2.4	27.8	Ø15/15	151.4|181.3
8	SHR [8]	1.00	300	370	2.2	25.0	Ø20/15	144.7| -
9	Hody [10]	1.00	280	500	2.2	25.0	Ø20/20	225.2|215.8
10	SHR [8]	1.00	300	370	3.3	56.1	Ø15/15	224.2|226.8
11	Hody [10]	1.00	280	500	3.3	56.1	Ø15/20	259.3| -
12	C70 [9]	1.00	300	460	2.6	31.0	Ø15/18 u	- | 190.7
13	ComFlor 80	1.00	280	690	2.6	31.0	Ø15/30 u	270.4|244.0
14	SHR [8]	0.75	250	370	2.5	30.4	Ø15/15	168.7|120.3
15	C70 [9]	1.00	250	460	2.5	30.4	Ø15/18	146.2|163.1

u ≙ location of reinforcing steel in through with c_{nom} = 20 mm, - ≙ outlier

Four different metal sheets were tested, whereby re-entrant profiles were included as well as profiles with an open shape. Furthermore, parameters were varied specifically to investigate their influence on the bearing behaviour. The parameters are the thickness of the metal sheet, the ratio of longitudinal reinforcement, the concrete strength, the location of the reinforcing steel and the height of the slab. Table 1 gives an overview over the combinations of the parameters. Two tests were performed with each combination. The specimens were named using the following principle: shape of metal sheet – thickness of metal sheet – height of specimen – concrete compressive strength – additional longitudinal reinforcement.

2.2 Test Results

The shear failure of composite slabs with additional reinforcing steel is very different to the bearing behaviour according to shear of concrete slabs. To explain that, the observations during the test procedure are described on the example of test C70-1,00-300-C30/37-Ø15/18h-1. Therefore, the force-deflection-diagram is shown in figure 2 and in figure 3 different crack patterns are presented. At a shear force of 30 kN the first bending cracks occurred, which results in the first change of the stiffness in the force-deflection-curve. With increasing load further formation of bending cracks could be observed. At a shear force of about 110 kN the diagram shows a significant load drop, which is followed by the second change of stiffness. The picture in the middle of figure 3 shows that a new crack appeared. This crack reaches the uncracked compression zone and runs inclined, so it could be identified as the shear crack. Because the shear crack wasn't critical, the cylinder load could be increased. During the load increase the crack propagation was still stable and a third area with a constant gradient could be seen in the force-deflection-diagram. The last picture in figure 3 shows that the further crack development was concentrated near to the support, because it was the horizontal part of the shear crack. At a shear force of about 160 kN the deflection of the specimen increased and the failure occurred a short time later. The failure was characterised by the opening of the shear crack. In summary the force-deflection-curve could be divided into four areas. The first one is the uncracked condition, followed by the area characterised by the formation of bending cracks. The third area describes the formation of the horizontal part of the shear crack and the last area is the failure of the specimen. Compared to concrete specimens which fail suddenly the behaviour at failure is different. After the shear crack reaches the concrete compression zone, the crack formation is still stable and the load could be increased significantly.

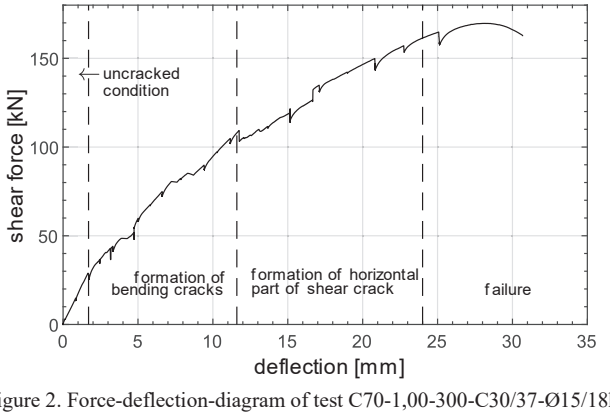

Figure 2. Force-deflection-diagram of test C70-1,00-300-C30/37-Ø15/18h-1.

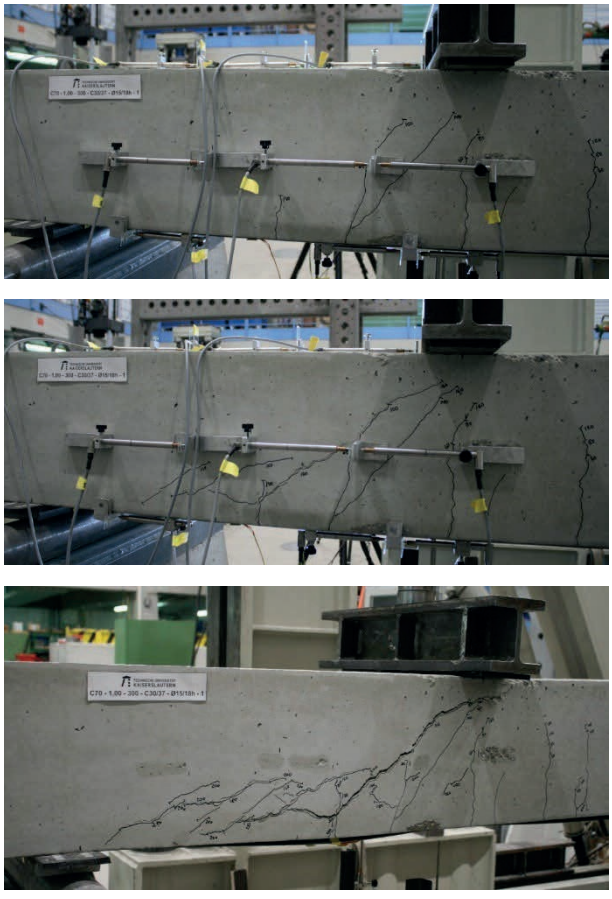

Figure 3. Crack patterns of test C70-1,00-300-C30/37-Ø15/18h-1
top: F_{cyl} = 140 kN, middle: F_{cyl} = 160 kN, bottom: Fracture pattern.

To investigate the crack pattern inside the specimens some selected ones were sliced. As an example, a picture of the longitudinal cut through the upper chord of the metal sheet of test C70-1,00-300-C30/37-Ø15/18h-1 is shown in figure 4. First of all, it is obvious that the crack pattern inside and outside the specimen differs. Only one crack is visible. It runs horizontal on the location of the smallest concrete width to the support. This observation was confirmed by the other sliced specimen. The oblique cracks on the outside of the specimen are the result of marginal influences.

Figure 4. Longitudinal cut through the upper chord of specimen C70-1,00-300-C30/37-Ø15/18h-1.

The strains of the metal sheets were continuous measured with glass fibre cables on the upper chord as well as on the lower chord. Thus, it could be determined, that at the location of the shear crack the strains of the lower chord reached their maximum where the strains on the upper chord reached their minimum. Contrary to the expectation the maximum strains in the metal sheet are not at the location of the maximum bending moment of the specimen. Furthermore, the concrete compressive strains on the top of the specimen were measured. Following the Bernoulli Hypothesis, the concrete strains should increase constantly from the support to the load introduction. On the contrary a steady increase could only be observed at the location of the shear crack. Then, the concrete compressive strains increased significantly with their maximum at the load introduction. These observations lead to the conclusion that the Bernoulli Hypothesis is not valid for the shear force bearing behaviour of composite slabs. When the shear crack occurs, the bearing behaviour changes to a tied arch model with two compression struts. The concrete in the location of the shear crack supports itself on the metal sheet, which results in the high measured strains. The second compression strut runs directly to the support.

3 NEW ENGINEERING MODEL

3.1 Basic description of the design model

From the observations in the tests and the continuous strain measurement by glasfibres a simplified truss model was developed. It is presented in figure 5. After the shear crack occurs the concrete supports itself on the metal sheet which transfers the shear force through the crack. Then, the dowel effect of the longitudinal reinforcement induces the forces back into the concrete. This is characterised by the tension strut in the truss model that brings the forces of the direct compression strut into the support. The horizontal tie which is necessary for the equilibrium is the longitudinal reinforcement.

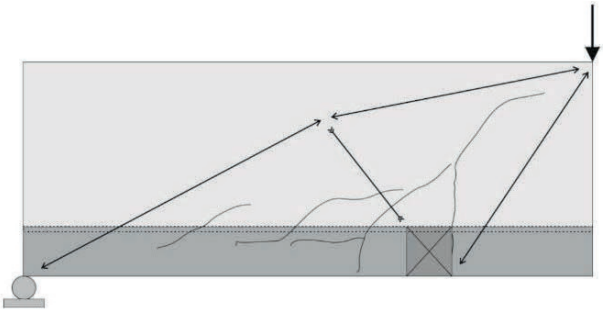

Figure 5. Truss model of shear transfer in composite slabs.

On the basis of the described truss model the engineering model for the design of the shear capacity of composite slabs with additional reinforcing steel was developed. The model is shown in figure 6 and contains four mechanisms that act additive. The shear transfer in the concrete compression zone $V_{c,cz}$, the shear transfer in the crack propagation zone $V_{c,ct}$ and the shear capacity of the tension strut that fails by kinking of the reinforcement or spalling of the concrete in the ribs $V_{c,ks}$ establish the equilibrium in the shear crack. In addition the vertical component of a strut that transfers the load to the support $V_{c,cs}$ is considered. The failure occurs when one of the mechanisms fails. The failure of the dowel effect of the reinforcement was identified as the kinematic condition for the overall failure of the specimen. Due to that the opening of the shear crack was possible which leads into the loss of the tensile bearing effects in the crack tip. The remaining two mechanisms cannot compensate these forces.

The strain measurement in the tension area showed that the metal sheet always reached the maximum tension bearing capacity in section II-II. Therefore, it is proposed to allocate the fully anchored tensile force to the metal sheet following the partial bond theory. The rest of the tension force, which is necessary for

the equilibrium of moments, should be referred to the reinforcing steel. Furthermore, the high utilisation of the metal sheet is the reason that the own shear capacity of the metal sheet is not considered in the described model.

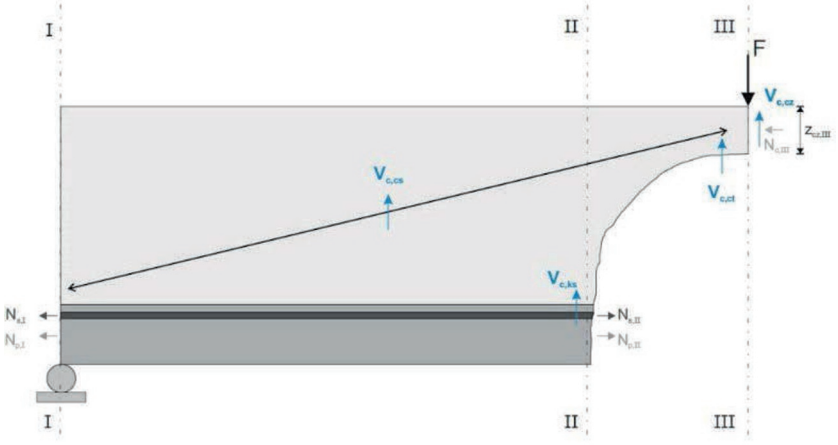

Figure 6. New shear design model for composite slabs with reinforcing steel.

3.2 Shear capacity of the uncracked compression zone $V_{c,cz}$

The shear capacity of the uncracked concrete compression zone $V_{c,cz}$ uses the height of the compression zone z_{pl}. This height depends on the tension forces in the steel sheet and the reinforcing steel in cross section II-II and the compression force in cross section III – III that represents the bending moment present in cross section III-III. The equation (1) was developed by Hartmeyer [6] with reference to Zink [11] and is assumed for this model. The factor 2/3 represents a parabolic distribution of the shear stresses in the concrete compression zone. It has to be noted that the use of a constant stress distribution of the normal stresses in the compression zone (see equation (2)) in combination with the parabolic distribution of the shear stresses is not consistent from the mechanical point of view. The use of a linear distribution of the normal stresses, which would be mechanically correct, is uncommon for composite constructions. In the interest of the Ease of Use this discrepancy is accepted.

Because the strain measurement with glasfibers showed that compared to the reinforcing steel the strains in the metal sheet were significantly higher, it is suggested to use the full anchored normal force of the metal sheet. The remaining forces necessary for the realisation of the bending moment should be assigned to the reinforcing steel.

$$V_{c,cz} = \frac{2}{3} \cdot z_{pl,III} \cdot b \cdot f_{ctm} \tag{1}$$

$$z_{pl,III} = \frac{N_{s,II}+N_{p,II}}{b \cdot f_{cm}} \tag{2}$$

3.3 Shear capacity of crack propagation zone $V_{c,ct}$

Hillerborg [12] introduced the critical length as a factor to describe the crack length that is able to transfer tensile stresses perpendicular to the crack. Hartmeyer [6] and Zink [11] used this approach to determine the shear capacity depending on the fracture energy G_f of the concrete. In this model the approach from Hartmeyer [6] was used and enhanced, s. equation (3).

$$V_{c,ct} = \alpha \cdot \beta \cdot l_{ch} \cdot b \cdot \frac{d_s}{d_{s,0}} = 0{,}12 \cdot \frac{G_f \cdot E_{cm}}{f_{ctm}} \cdot b \cdot \frac{d_s}{d_{s,0}} \quad (3)$$

The fracture energy is determined by the rules of Model Code 2010 [13]. The factors, which are necessary for the description of the characteristic length, were assumed from Remmel [14] and Grimm [15] (β = 0,4) and Reinhardt et al. [16] (α = 0,3). The length of the shear crack with small crack width is not only dependent on the material behaviour but also on the total length of the crack. Good results were received by using the basic formula on very thick slabs. For the application in thinner slabs a linear dependence of the effective crack length on the effective height d was assumed. The basic value $d_{s,0}$ limits this effect to the maximum height d_s for which experimental data exists. The linear proportionality is a simplified assumption.

The investigation of the crack patterns in the test showed that the shear crack runs nearly horizontal when reaching the uncracked compression zone. Therefore, the consideration of the angle of the shear crack is not necessary.

3.4 Shear capacity inducing kinking and spalling $V_{c,ks}$

Two failure modes has to be considered, concrete failure $V_{c,ks,1}$ and steel failure $V_{c,ks,2}$, where the one with the lowest shear capacity should be used for the mechanism $V_{c,ks}$ according to equation (4).

$$V_{c,ks} = min\begin{cases} V_{c,ks,1} \\ V_{c,ks,2} \end{cases} \quad (4)$$

For the shear capacity inducing spalling the approach from Baumann and Rüsch [17] was enhanced according to equation (5). In figure 4 a horizontal crack can be found. As explained this crack occurs in all test specimen and it is located at the minimum width between shear connectors in the webs of the steel sheets. The width $b_{min,bar}$ has to be taken as the minimum width described above minus the diameter of the longitudinal reinforcement. Baumann and Rüsch [17] introduced a length d_{eq} in their formula which was adapted here to the height h_{pc}. For all types of steel sheets with shear connectors in the webs the height of the lowest connector above the bottom chord of the sheet is taken as h_{pc}. It is assumed that in other cases with re-entrant profiles h_{pc} is the middle between the upper and lower chord which both introduce shear by contact forces perpendicular to the span. The geometry values b_{min} and h_{pc} are explained in figure 7. In [17] the third square root of the concrete compressive strength was used to take the concrete tensile strength into account. Equation (5) shows that the concrete tensile strength is here considered directly with f_{ctm}.

$$V_{c,ks,1} = 1{,}64 \cdot b_{min,bar} \cdot h_{pc} \cdot f_{ctm} \quad (5)$$

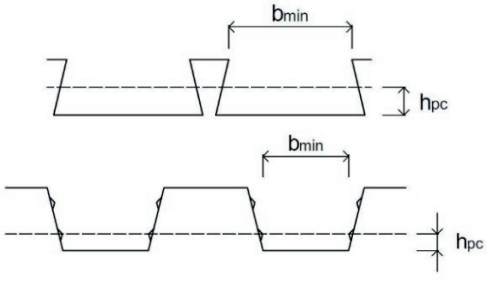

Figure 7. Geometry values b_{min} and h_{pc}.

The equations for the kinking resistance of the longitudinal reinforcement were taken from Model Code 2010 [13], see equation (6). Factor η_s is the utilization ratio of the reinforcing steel. As mentioned before, in all tests we observed that the utilization of the steel sheet was significantly higher than that of the reinforcement. Therefore, we propose that first the full utilization of the steel sheet in the decisive section

is assumed and then the remaining tensile force is used to determine the utilization of the reinforcement. Furthermore, the approach in [13] contains a formulation dependent on the displacement of the crack origins. With a displacement of $0{,}2 \cdot d_s$ the maximum dowel effect can be activated. This formulation represents a criterion of serviceability. Because on the one hand the design of the shear force bearing behaviour belongs to ULS and on the other hand in the tests crack displacements in the range of $0{,}2 \cdot d_s$ could be observed the expression depending on displacement could be neglected.

$$V_{c,ks,2} = 1{,}6 \cdot A_s \cdot \sqrt{f_{sk}} \cdot \sqrt{f_{cm}} \cdot \sqrt{1 - \eta_s^2} \tag{6}$$

3.5 Shear capacity of the direct compression strut $V_{c,cs}$

The vertical component of the direct compression strut is another component of the shear capacity of composite slab in those cases where a strut can directly anchor on a direct support. The direct compression strut is at equilibrium with the anchored tension force in section I-I, so the vertical component has to be calculated according equation (7). In correspondence to concrete members the inclination angle of the compression strut is named θ.

$$V_{c,cs} = \left(N_{s,I} + N_{p,I}\right) \cdot \tan\theta \tag{7}$$

In all test specimen the slabs were longer than the span so an overhanging length of about 500 mm was used to anchor the tension forces in the steel sheet and in the reinforcement. Due to the fact, that the bending moment at the support is about zero (just a small hogging moment out of dead weight of the slab) it is absolutely necessary that there has to be some bending moment in the concrete slab to reach this equilibrium. In some tests some minor cracks have been detected at to top side of the composite slab in the region of the support at ULS. Therefore, it is assumed as a simplification that the stresses in the concrete have a triangular shape with a concrete stress about zero at the top edge of the slab, see figure 8. This leads to the simplified assumption that the position of the direct compression strut is located at 1/3 of the height of the slab. For rectangular members this approach is correct. But in composite slabs the concrete in the area of the metal sheet is constricted, which has to be considered by determining z_{SP} as position of the centroid of compression stresses.

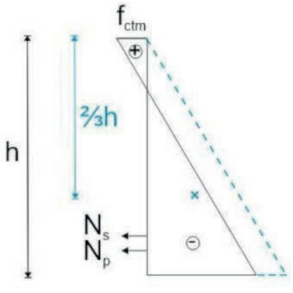

Figure 8. Stress distributions in concrete in section I-I.

At its opposite end the direct compression strut begins at the uncracked compression zone above the shear crack. In all test specimen this strut started at the load introduction into the specimen. So, the inclination angle could be determined according to equation (8), where z_{pl} has to be determined with the tension forces in section II – II of figure 6.

$$\tan\theta = \frac{z_{SP} - 0{,}5 \cdot z_{pl,III}}{3 \cdot d_m} \tag{8}$$

Because of the dependency of the shape of the metal sheet the calculation of tan θ is time consuming. Therefore, a parameter study was done to provide a simplified assumption of tan θ. For the parameter study common cross sections of decks were used. The applied loads were chosen that high that the cross sections reached their bending capacity. Due to that the height of the uncracked compression zone increases and the inclination angle of the compression strut decreases. Figure 9 shows the results of the parameter study. For the simplified assumption of tan θ the value 0.21 was chosen as the minimum value. In general, for thinner decks in combination with higher concrete compressive strength greater values could be observed. Because higher concrete compressive strength are rarely used in composite slabs and the use of formula (8) is time-consuming, tan θ = 0.21 is a satisfied assumption.

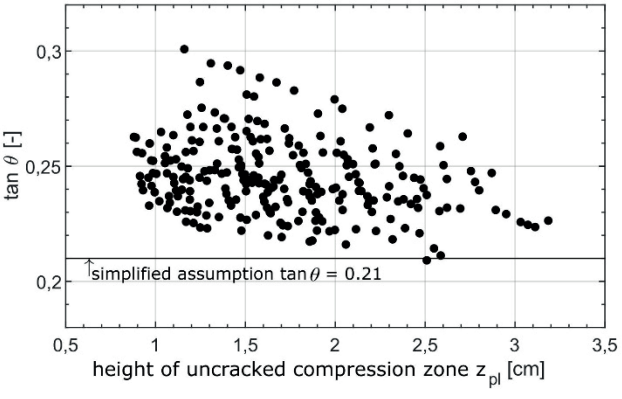

Figure 9. Results of parameter study to tan θ.

4 VERIFICATION AND STATISTICAL ANALYSIS OF THE DESIGN MODEL

With the developed model the shear force capacity could be calculated depending on the bending load. So, the model is very different to the current model [2] which describes the shear force capacity of a cross section of a bending member. Like described above three of the mechanisms are depending on the utilisation ratio of the longitudinal reinforcement. Thus, an independent consideration is not possible.

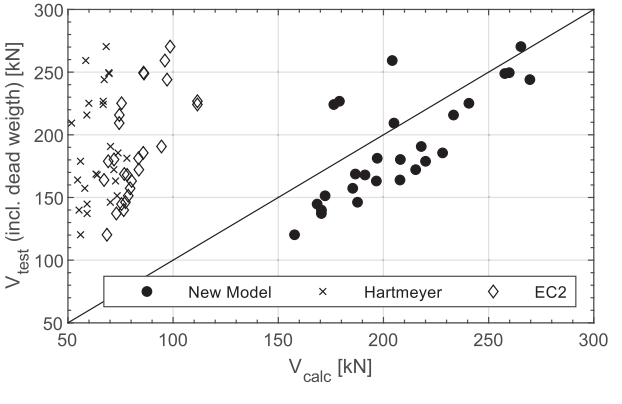

Figure 10. Comparative presentation of test results with calculated shear forces as mean values.

Figure 10 shows the plot of ultimate load in the tests V_{test} vs. the ultimate load according the developed design model V_{calc}. It shows a very good accordance between the tests and the model. Furthermore, the accordance is independent from the shape of the metal sheet. Also plotted in figure 10 are the comparisons between the test results and the shear forces calculated with the model of the current EN 1992 [2] and the model of Hartmeyer [6]. It becomes clear that with these models the shear force capacity of composite slabs cannot be described reliable. Even though the capacities are on the safe side, only with the new developed model the capacities can be calculated economical. Table 2 contains the values describing the mathematical reliability of the models. The new developed model is considered in the draft of Eurocode 4 [18].

Table 2: Comparison of test results with calculated shear forces as mean values.

Design Model	Mean Value	Standard deviation	Coefficient of determination
New Model	0,918	0,141	0,572
Eurocode 2 [2]	2,296	0,387	0,412
Hartmeyer [6]	3,001	0,676	0,031

The recalculation of the tests with the developed model was done at the location of the shear crack. Because the prediction of the location of the shear crack isn't possible at that time in practice the calculation of the shear force capacity has to be done in the given section in the distance d from the support. The model was statistical analysed and the mean values of the material strength were transferred into characteristic values. With a safety factor of γ_R = 1,3 the design value of the shear force capacity could be calculated according equation (9). The equations for the calculation of the mechanisms on the characteristic level are summarised in table 3.

$$V_{Rd} = \frac{0{,}694}{\gamma_R} \cdot \left[V_{c,cz} + V_{c,ct} + V_{c,ks} + V_{c,cs}\right] \tag{9}$$

Because with the developed model the calculation of the normal forces in different sections is necessary for the calculation of the shear force capacity the question arises whether the model could be simplified for the Ease of Use in practice. Therefore, a simplified design check is proposed. Only the tensile forces in the section of the support has to be calculated and used for the calculation of the different mechanisms. The tension force at support is at equilibrium with the compression force in the known distance d from the support. A verification of this approach was done with different statistical analysis. More information can be found in [19].

Table 3: Summary of equations for the calculation of the design shear force capacity.

Mechanism	Calculation
Compressive zone	$V_{c,cz} = \frac{2}{3} \cdot z_{pl} \cdot b \cdot f_{ctm}$
	with: $z_{pl} = \frac{N_{s,II}+1{,}15 \cdot \tau_{rk} \cdot b \cdot L_{II}}{1{,}33 \cdot b \cdot f_{ck}}$
	z_{pl} = height of uncracked compression zone f_{ctm} = mean value of cylinder tensile strength of concrete $N_{s,II}$ = normal force in reinforcing steel in section II-II τ_{rk} = characteristic value of longitudinal shear stress of metal sheet L_{II} = horizontal distance between section I-I and II-II f_{ck} = characteristic cylinder compressive strength of concrete
Crack propagation zone	$V_{c,ct} = 0{,}12 \cdot \frac{G_f \cdot E_{cm}}{f_{ctm}} \cdot b \cdot \frac{d_s}{d_{s,0}}$
	with: $G_f = 73 \cdot f_{cm}^{0,18}$ fcm [N/mm²]
	G_f = fracture energy of concrete [N/m] E_{cm} = mean value of Young`s modulus d_s = effective height of reinforcing steel $d_{s,0}$ = basic value of effective height of reinforcing steel = 270 mm
Dowel effect	$V_{c,ks} = \min\{V_{c,ks,1}; V_{c,ks,2}\}$
	with: $V_{c,ks,1} = 1{,}64 \cdot b_{min} \cdot h_{pc} \cdot f_{ctm}$
	b_{min} = minimum width of concrete inside of the metal sheet h_{pc} = vertical distance between bottom edge of metal sheet and the lowest shear connector $V_{c,ks,2} = 1{,}6 \cdot A_s \cdot \sqrt{f_{sk}} \cdot \sqrt{f_{ck}} \cdot \sqrt{1-\eta_s^2}$ A_s = cross section of reinforcing steel f_{sk} = characteristic value of yield strength of reinforcing steel η_s = utilisation ratio of reinforcing steel
Direct compression strut	$V_{c,cs} = \tan\theta \cdot (N_{s,I} + N_{p,I})$
	with: $\tan\theta = \frac{z_{SP}-0{,}5 \cdot z_{pl}}{3 \cdot d_m}$
	$N_{p,I} = 1{,}15 \cdot \tau_{rk} \cdot b \cdot L_I$ θ = inclination angle of compression strut $N_{s,I}$ = normal force of reinforcing steel in section I-I $N_{p,I}$ = normal force of metal sheet in section I-I z_{SP} = location of compression strut from the top edge of deck d_m = mean value of effective heitgh L_I = bond length of metal sheet behind the support

REFERENCES

[1] DIN EN 1994-1-1 2010, *Eurocode 4: Bemessung und Konstruktion von Verbundtragwerken aus Stahl und Beton – Teil 1-1: Allgemeine Bemessungsregeln und Anwendungsregeln für den Hochbau, Deutsche Fassung EN 1994-1-1:2004 + AC:2009*, Beuth, Berlin.

[2] DIN EN 1992-1-1 2010, *Eurocode 2: Bemessung und Konstruktion von Stahlbeton- und Spannbetontragwerken – Teil 1-1: Allgemeine Bemessungsregeln und Regeln für den Hochbau, Deutsche Fassung EN 1992-1-1:2004 + AC:2010*, Beuth, Berlin.

[3] Reineck, K.-H., *Ein mechanisches Modell für den Querkraftbereich von Stahlbetonbauteilen*, Dissertation, Universität Stuttgart, 1990.

[4] Reineck, K.-H., Kuchma, D.A. und Fitik, B., "Erweiterte Datenbanken zur Überprüfung der Querkraftbemessung für Konstruktionsbauteile mit und ohne Bügel", *DAfStb-Heft 597*, 2012.

[5] Brüdern, A.-E., Mechtcherine, V., Kurz, W. and Jurisch, F., "Self-Compacting Lightweigth Aggregate Concrete for Composite Slabs", *Proceedings of Advanced Concrete Materials International Conference*, Stellenbosch, South-Africa, 2009.

[6] Hartmeyer, S., *Modell zur Beschreibung des Querkrafttragverhaltens von Stahlverbunddecken aus Leicht- und Normalbeton*, Dissertation, Technische Universität Kaiserslautern, 2014.

[7] Z-12.5-96, *Allgemeine bauaufsichtliche Zulassung Z-12.5-96 – Ankerstabstahl St 900/1100 mit Geweinderippen AWM 1100 Nenndurchmesser: 15 und 20 mm, Stahlwerk Annahütte Max Aicher GmbH & Co. KG, 01.10.2015 – 01.10.2020,* Berlin, 2015.

[8] Z-26.1-45, *Allgemeine Bauartgenehmigung Z-26.1-45 – SUPER-HOLORIB SHR 51-Verbunddecke, Montana Bausysteme AG, 13.03.2018 – 13.08.2023*, Berlin, 2018.

[9] Z-26.1-22, *Allgemeine bauaufsichtliche Zulassung Z-26.1-22 – COFRASTRA Verbunddecken, ArcelorMittal Construction Deutschland GmbH, 28.07.2016 – 28.07.2021*, Berlin, 2016.

[10] Z-26.1-52, *Allgemeine Bauartgenehmigung Z-26.1-52 – Verbunddecke Hody SB 60, REPPEL b.v. Bouwspecialiteiten, 01.07.2019 – 01.07.2024*, Berlin, 2019.

[11] Zink, M., *Zum Biegeschubversagen schlanker Bauteile aus Hochleistungsbeton mit und ohne Vorspannung*, Dissertation, Universität Leipzig, 2000.

[12] Hillerborg, A. "Analysis of one Single Crack", *Fracture Mechanics of Concrete*, 1983.

[13] Model Code *Model Code 2010 – First complete draft, Volume 1*, Lausanne: International Federation for Structural Concrete (fib), 2010.

[14] Remmel, G., "Zum Zug- und Schubtragverhalten von Bauteilen aus hochfestem Beton", *DAfStb-Heft 444*, 1994.

[15] Grimm, R., "Einfluß bruchmechanischer Kenngrößen auf das Biege- und Schubtragverhalten hochfester Betone", *DAfStb-Heft 447*, 1997.

[16] Reinhardt, H.-W., Cornelissen, H., Hordijk, D.A., "Tensile Tests and failure Analysis of Concrete", *Journal of Structural Engineering*,112(11), 2462-2477, 1986.

[17] Baumann, T., Rüsch, H., "Versuche zum Studium der Verdübelungswirkung der Biegezugbewehrung eines Stahlbetonbalkens" *DAfStb-Heft 210*, 1970.

[18] prEN 1994-1-1, *Eurocode 4: Design of composite steel and concrete structures – Part 1-1: General rules and rules for buildings – SC4.T6: Draft prEN 1994-1-1:042020 + comments*. CEN European Committee for Standardization.

[19] Schmeckebier, N. *Ein Ingenieurmodell zur Berechnung der Querkrafttragfähigkeit von Stahlverbunddecken des Hochbaus mit praxisrelevanter Betonstahlbewehrung*, Dissertation, Technische Universität Kaiserslautern, 2021.